

Autoassociative Memory Retrieval and Spontaneous Activity Bumps in Small-World Networks of Integrate-and-Fire Neurons

Anastasia Anishchenko*

Department of Physics and Brain Science Program
Brown University, Providence RI 02912, USA

Elie Bienenstock

Division of Applied Mathematics,
Department of Neuroscience, Brain Science Program
Brown University, Providence RI 02912, USA

Alessandro Treves

Cognitive Neuroscience
SISSA - International School for Advanced Studies
Via Beirut 4, 34014 Trieste, Italy

October 31, 2018

*E-mail: anish@physics.brown.edu

Abstract

The metric structure of synaptic connections is obviously an important factor in shaping the properties of neural networks, in particular the capacity to retrieve memories, with which are endowed autoassociative nets operating via attractor dynamics. Qualitatively, some real networks in the brain could be characterized as 'small worlds', in the sense that the structure of their connections is intermediate between the extremes of an orderly geometric arrangement and of a geometry-independent random mesh. Small worlds can be defined more precisely in terms of their mean path length and clustering coefficient; but is such a precise description useful to better understand how the type of connectivity affects memory retrieval?

We have simulated an autoassociative memory network of integrate-and-fire units, positioned on a ring, with the network connectivity varied parametrically between ordered and random. We find that the network retrieves when the connectivity is close to random, and displays the characteristic behavior of ordered nets (localized 'bumps' of activity) when the connectivity is close to ordered. Recent analytical work shows that these two behaviours can coexist in a network of simple threshold-linear units, leading to localized retrieval states. We find that they tend to be mutually exclusive behaviours, however, with our integrate-and-fire units. Moreover, the transition between the two occurs for values of the connectivity parameter which are not simply related to the notion of small worlds.

1 Introduction

Autoassociative memory retrieval is often studied using neural network models in which connectivity does not follow any geometrical pattern, – i.e. it is either all-to-all or, if sparse, randomly assigned. Such networks can be characterized by their storage capacity, expressed as the maximum number of patterns that can be retrieved, which turns out to be proportional to the number k of connections per unit. Networks with a regular geometrical rule informing their connectivity, instead, can often display geometrically localized patterns of activity, i.e. stabilize into activity profile 'bumps' of width proportional to k . Recently, applications in various fields have used the fact that small-world networks, characterized by a connectivity intermediate between regular and random, have different graph theoretic properties than either regular or random networks. In particular, small-worlds have both a high clustering coefficient C and a short characteristic path length L , at the same time [19].

Note that while autoassociative retrieval is an obvious model for a physiological memory process, also self-sustaining localized states are of interest for the real brain, as models of the short-term memory of a location on a cortical map. The two behaviours are combined in models of cortical function in which a localized and input-specific pattern of activity represents the memory of a given stimulus in a given position on the sensory array [15].

Here we consider a family of 1D networks of integrate-and-fire units, where changing the parameter of randomness q allows to go from a regular network ($q = 0$) in which all connections are relatively short-range, to a spatially random network ($q = 1$) in which all connections can be considered to be long-range. Intermediate values of q correspond to a biologically plausible combination of long- and short-range connections. For $q = 0$ such a network spontaneously forms activity bumps [4], and this property is expected to be preserved at least for small values of q . For $q = 1$ the network behaves as an ordinary autoassociative net [1, 8], and likewise this is expected to hold also for $q < 1$, as it does with a simpler binary-unit model [12].

Can activity bumps and retrieval coexist?

We first explore how both the ability to retrieve, and to form bumps, change with the degree of randomness q in the connectivity. Recent analytical work, on a model in which the connectivity has a Gaussian spread of variable width, in fact shows that retrieval and localization coexist below a critical width value (and a critical storage load) [13]. We can then address the question of whether the two abilities can coexist also with our connectivity model, at least in an intermediate regime between $q \simeq 0$ and $q \simeq 1$.

Is the transition between the different regimes related to small worlds?

Since the ability to form bumps depends on the mutual support among active units through excitatory feedback loops, one can expect it to persist as long as the clustering coefficient C remains large, even as q grows above 0. Conversely, since pattern retrieval depends on the propagation of the retrieval signal to all units in the network independently of their location, one can expect robust retrieval to require that the mean path length from one unit to any other one is

still short, even if q is below 1. Thus, one can expect an intermediate small-world regime of coexistence between bumps and retrieval.

Can they coexist in more realistic networks, with integrate-and-fire dynamics?

Bohland and Minai [6], and more recently McGraw and Menzinger [10] and Morelli et al [12] have considered somewhat related issues with model networks of binary neurons, in which localization and retrieval do not appear to coexist (an observation explained by a simple argument proposed by Yasser Roudi (personal communication)). By contrast, Roudi and Treves find that they coexist with threshold-linear units [13]. The essential difference between these two very simple and dynamically implausible models, for the stability of bump states and of retrieval states, is whether single-unit activity levels saturate or not. Integrate-and-fire units with an absolute refractory period saturate to an intermediate and variable degree (depending, effectively, on how far below saturation they normally operate [1, 14]). They provide therefore a dynamically more plausible, but still very simple model to approach the issue of the coexistence of localization and retrieval in a cortical setting. This is what we discuss here, presenting the result of computer simulations.

2 Model

2.1 Integrate-and-Fire Model

We consider a family of 1D networks of N integrate-and-fire units [17], arranged on a ring. In the simplest possible integrate-and-fire model we adopt, the geometry of a neuron is reduced to a point, and the time evolution of the membrane potential V_i of cell i , $i = 1, \dots, N$ during an interspike interval follows the equation

$$\frac{dV_i(t)}{dt} = -\frac{V_i(t) - V^{res}}{\tau_m} + \frac{R_m}{\tau_m} (I^{syn}(t) + I^{inh}(t) + I_i(t)) \quad (1)$$

where τ_m is the time constant of the cell membrane, R_m its passive resistance, and V^{res} the resting potential. The total current entering cell i consists of a synaptic current $I_i^{syn}(t)$ due to the spiking of all other cells in the network that connect to cell i , an inhibitory current $I^{inh}(t)$, which depends on the network activity, and a small external current $I_i(t)$, which represents all other inputs into cell i .

The last, external component of the current can be expressed through a dimensionless variable $\lambda_i(t)$ as

$$I_i(t) = \lambda_i(t)(V^{th} - V^{res})/R_m \quad (2)$$

We use a simplified model for the inhibition, where it depends on the excitatory

activity of the network. The inhibitory current is the same for all neurons at a given moment of time, and changes in time according to the equation

$$\frac{dI^{inh}(t)}{dt} = -\frac{1}{\tau_{inh}}I^{inh}(t) + \lambda^{inh}\frac{(V^{th} - V^{res})}{NR_m}r(t) \quad (3)$$

where λ^{inh} is a dimensionless inhibitory parameter of the model and $r(t)$ is a rate function characterizing the network activity up to time t :

$$r(t) = \sum_i \sum_{\{t_i\}} \int_{-\infty}^t K(t-t')\delta(t'-t_i)dt' \quad (4)$$

The kernel $K(t-t')$ we use for our simulations is a square wave function lasting one time step Δt of the integration, so that $r(t)$ is just a total number of spikes in the time interval Δt .

As V_i reaches a threshold value V^{thr} , the cell emits a spike, after which the membrane potential is reset to its resting value V^{res} and held there for the duration of an absolute refractory period τ_{ref} . During this time the cell cannot emit further spikes no matter how strongly stimulated.

2.2 Synaptic Inputs

All synapses between neurons in the network are excitatory, and the synaptic conductances are modeled as a difference of two exponents with time constants τ_1 and τ_2 , such that τ_2 is of the order of τ_m and $\tau_1 \gg \tau_2$. The synaptic current entering cell i at time t then depends on the history of spiking of all cells that have synapses on i :

$$I_i^{syn}(t) = \frac{\tau_m}{R_m} \sum_{j \neq i} \sum_{\{t_j\}} \frac{\Delta V_{ji}}{\tau_1 - \tau_2} \left(e^{-\frac{t-t_j}{\tau_1}} - e^{-\frac{t-t_j}{\tau_2}} \right) \quad (5)$$

where $\{t_j\}$ are all the times before time t when neuron j produced a spike and ΔV_{ji} is a size of the excitatory postsynaptic potential (EPSP) in neuron i evoked by one presynaptic spike of neuron j .

The relative size of the evoked EPSP determines the efficacy of synapse ji :

$$\Delta V_{ji} = \lambda^{syn} \frac{(V^{th} - V^{res})}{N} c_{ji} [1 + J_{ji}] \quad (6)$$

where λ^{syn} is the model parameter characterizing synaptic excitation, c_{ji} is 0 or 1 depending on the absence or presence of the connection from neuron j to neuron i , and J_{ij} is modification of synaptic strength due to Hebbian learning, which will be described later (Section 2.4).

2.3 Connectivity

In our model, all connections in the network are uni-directional, so the connectivity matrix is not symmetrical. We use a special procedure for creating connections, after [19]: the probability of one neuron to make a connection to another depends on a parameter q in such a way, that changing q from 0 to 1 allows one to go from a regular to a spatially random network.

A regular network ($q = 0$) in this case is a network where connections are formed based on a Gaussian distribution. The probability to make a connection from neuron i to neuron j in such a network is

$$P_0(c_{ij}) = e^{-\frac{|i-j|^2}{2\sigma^2}} \quad (7)$$

where $|i - j|$ is the minimal distance between neurons i and j on the ring. This results in an average number of connections per neuron $k \approx \sqrt{2\pi}\sigma$ (actually, $k < \sqrt{2\pi}\sigma$ because of the finite length of the ring).

In a random network ($q = 1$), the probability of creating a connection does not depend on the distance between neurons:

$$P_1(c_{ij}) = k/N \quad (8)$$

Intermediate values of q thus correspond to a biologically plausible combination of long- and short-range connections:

$$P_q(c_{ij}) = (1 - q)e^{-\frac{|i-j|^2}{2\sigma^2}} + q\frac{k}{N} \quad (9)$$

The parameter q is referred to as the ‘randomness’ parameter, following Watts and Strogatz, who used a similar procedure for interpolating between regular and random graphs.

As originally analyzed by Watts and Strogatz[19], the average path length and clustering coefficient in a graph wired in this way both decrease with q , but their functional dependence takes different shapes. Thus, there is a range of q where the clustering coefficient still remains almost as high as it is in a regular graph, while the average path length already approaches values as low as for random connectivity. Graphs that fall in this range are called small-world graphs, referring to the fact that for the first time this type of connectivity was explored in a context of social networks [11]. In this context the average (or characteristic) path length L can be thought of as the average number of friends in the shortest chain connecting two people, and the clustering coefficient C as the average fraction of one’s friends who are also friends of each other.

In a neural network, L corresponds to the average number of synapses that need to be passed in order to transmit a signal from one neuron to another, and thus depends on the number and distribution of long-range connections. The

clustering coefficient C characterises the density of local connections, and can be thought of as the probability of closing a trisynaptic loop (the probability that neuron k is connected to i , given that some neuron j which receives from i connects to k).

2.4 Hebbian plasticity

Associative memory in the brain can be thought of as mediated by Hebbian modifiable connections. Modifying connection strength corresponds to modifying the synaptic efficacy of Eq. 6:

$$J_{ij} = \frac{1}{M} \sum_{\mu=1}^p \left(\frac{\eta_i^\mu}{\langle \eta \rangle} - 1 \right) \left(\frac{\eta_j^\mu}{\langle \eta \rangle} - 1 \right) \quad (10)$$

where η_i^μ is the firing rate of neuron i in the μ th memory pattern, $\langle \eta \rangle$ is the average firing rate, the network stores p patterns with equal strength, and M is a normalization factor. The normalization factor should be chosen to maximally utilize the useful range of synaptic efficacy, which could be done by equalizing its variance with its mean. In order to preserve the non-negativity of each efficacy, in Eq. 6 we set $J_{ij} = -1$ whenever $(1 + J_{ij}) < 0$.

We draw patterns of sparseness a from a binary distribution, so that $\eta_i^\mu = 1/a$ with probability a and $\eta_i^\mu = 0$ with probability $1 - a$. The 'average firing rate' $\langle \eta \rangle$ in this case is equal to 1.

2.5 Experimental Paradigm

After the connections have been assigned and the synaptic efficacies modified by storing memory patterns, we randomize the starting membrane potentials for all the neurons:

$$V_i^{st} = V^{res} + \beta(V^{th} - V^{res})n_i \quad (11)$$

where $\beta = 0.1$ is a constant and n_i is a random number between 0 and 1, generated separately for each neuron i . We then let the network run its dynamics.

After a time t_0 , a cue for one of the p patterns (for instance, pattern μ) is given, in the form of an additional cue current injected into each cell. The cue current is injected at a constant value up to the time t_1 , and then decreased linearly to 0 so that it becomes 0 at time t_2 . Thus, for the dimensionless current in (2) we have

$$\lambda_i(t) = \lambda^0 + \lambda^{cue} f(t)(\eta_i^\mu - 1) \quad (12)$$

where $\lambda^0 > 0$ is a constant, dimensionless external current flowing into all cells, λ^{cue} is a dimensionless cue current parameter, and

$$f(t) = \begin{cases} 0 & : t < t_0 \text{ or } t_2 \leq t \\ 1 & : t_0 \leq t < t_1 \\ 1 - \frac{t-t_1}{t_2-t_1} & : t_1 \leq t < t_2 \end{cases} \quad (13)$$

If the cue is partial – for example, the cue quality $\rho = 25\%$ – then a continuous patch of the network, comprised of 25% of the length along the network ring, receives the cue for pattern μ , whereas the rest of the network receives a random pattern. (In the simulations, the random pattern on the rest of the network has a higher average activity than the original patterns, which makes the overall network activity rise slightly during application of the cue.)

During the time t_{sim} of the simulation, spike counts (numbers of spikes fired by each neuron), are collected in sequential time windows of length t_{win} :

$$r_i(t) = \sum_{\{t_i\}} \int_{t-t_{win}}^t \delta(t' - t_i) dt' \quad (14)$$

We then look at the geometrical shape of the network activity profile in each window, and at the amount of overlap of this activity with each of the patterns stored.

The amount of overlap with pattern μ in the time window ending at time t is calculated as the cosine of the angle between the pattern and the spike count vector:

$$O^\mu(t) = \frac{\sum_i \eta_i^\mu r_i(t)}{\sqrt{\sum_i [\eta_i^\mu]^2 \times \sum_i [r_i(t)]^2}} \quad (15)$$

The measure of memory retrieval is

$$m = \frac{1}{p} \sum_{\mu=1}^p \left[\frac{O^\mu(t_{sim}) - O_{chance}^\mu(t_{sim})}{1 - O_{chance}^\mu(t_{sim})} \right] \quad (16)$$

where $O_{chance}^\mu(t)$ is the chance level of the overlap when the cue for pattern μ is given:

$$O_{chance}^\mu(t) = \frac{1}{p-1} \sum_{\mu' \neq \mu} O^{\mu'}(t) \quad (17)$$

Note that the retrieval measure m may occasionally become negative. This occurs when retrieval is so poor that, even though a cue for pattern μ has been given, the network activity happens to have less overlap with μ than it has, on average, with the other stored patterns.

To quantify the prominence of the bump in the network activity profile, we compute the standard deviation of the position of each neuron weighted by its activity, with respect to the center of mass of the activity profile:

$$\sigma_a(t) = \sqrt{\frac{\sum_i |i - i_{CM}|^2 r_i(t)}{\sum_i r_i(t)}} \quad (18)$$

The ratio of the standard deviation σ_0 of a uniform distribution to $\sigma_a(t)$ has an intuitive meaning as the number of bumps that can be fit on the ring next to each other. We take the measure of 'bumpiness' to be

$$b(t) = \frac{\frac{\sigma_0}{\sigma_a(t)} - 1}{\frac{N}{k} - 1} \quad (19)$$

For an easier comparison with the memory retrieval measure, we compute the 'bumpiness' of a particular network in the last time window of the simulation ($t = t_{sim}$), and then average over simulations with different cues.

A rough measure of the relevance of saturation effects to the activity of single units is the ratio ψ between the firing rate of the most active units in a localized state or in a retrieval state, and their maximum possible firing rate, given by the inverse of the absolute refractory period. In fact, for binary units $\psi = 1$ and for threshold-linear units $\psi = 0$. In our simulations, the most active units typically fired at 120 *Hz* and the absolute refractory period was 3 *msec*, implying $\psi \simeq 0.3$.

Table 1: Parameters Used for the Simulations.

Quantity	Symbol	Value
Number of cells	N	1000
Average number of outgoing connections per cell	k	24 - 208
Parameter of randomness	q	0 - 1
Synaptic excitation constant	λ^{syn}	40
Inhibition constant	λ^{inh}	20
External excitatory current parameter	λ^0	0.25
Cue current parameter	λ^{cue}	0.1
Number of memory patterns stored	p	5
Memory sparseness	a	0.2
Synaptic plasticity normalization factor	M	10
Cue quality	ρ	5 - 100%
Membrane time constant	τ_m	5 msec
Synaptic conductance time constant 1	τ_1	30 msec
Synaptic conductance time constant 2	τ_2	4 msec
Inhibition time constant	τ_{inh}	4 msec
Absolute refractory period	τ_{ref}	3 msec
Integration time step	Δt	0.1 msec
Simulation time	t_{sim}	1000 msec
Cue onset time	t_0	150 msec
Time when the cue starts to decrease	t_1	300 msec
Cue offset time	t_2	500 msec
Sampling time window	t_{win}	50 msec

Note: Ranges are indicated for quantities that varied within runs.

3 Results

3.1 Graph-Theoretic Properties of the Network

Finding an analytical approximation for the characteristic path length L is not a straightforward calculation. Estimating the clustering coefficient C for a given network is, however, quite easy. In our case, integrating connection probabilities (assuming, for the sake of simplicity, an infinite network) yields the analytical estimate

$$C(q) = \left[\frac{1}{\sqrt{3}} - \frac{k}{N} \right] (1 - q)^3 + \frac{k}{N} \quad (20)$$

or, after normalization,

$$C'(q) = \frac{C(q) - C_{min}}{C_{max} - C_{min}} = (1 - q)^3 \quad (21)$$

which does not depend either on the network size N , or on the number k of connections per neuron.

Once connections have been assigned, both L and C can be calculated numerically. Keeping the number of connections per neuron $k > \ln N$ ensures that the graph is connected [7], i.e. that the number of synapses in the shortest path between any two neurons does not diverge to infinity.

The results of numerical calculations are shown in Fig. 1A. The characteristic path length and the clustering coefficient both decrease monotonically with q , taking their maximal values in the regular network and minimal values in the random network. Similar to what was described by Watts and Strogatz[19][18], L and C decrease in different fashions, with L dropping down faster than C . For example, for $q = 0.2$, C' is at 52% of its maximal value $C'(0) \equiv 1$, while $L - L_{min}$ has already dropped to 8% of $L(0) - L_{min}$. The inset shows that L approaches its maximal value $L(0)$ only for $q < 10^{-4}$.

Comparing the clustering coefficient estimated analytically with the simplified formula (20) and the one calculated numerically shows some minor discrepancy (Fig. 1B), which is due to the fact that analytical calculations were performed for an infinite network.

In conclusion, over a broad range $0.001 \leq q \leq 0.2$ one can characterize the mean path length as short, and the clustering coefficient as large, and one can therefore expect simulations with e.g. $q = 0.05$ or $q = 0.1$ to demonstrate characteristic small-world behaviour.

3.2 Bumps Formation in a Regular Network

Networks whose connectivity follows a strict geometrical order spontaneously form bumps in their activity profile, as shown in Fig. 2. Bumps are formed before the presentation of a pattern specific cue, and can either persist, or be temporarily or permanently altered or displaced after cue onset. Robust bumps, which remain after the cue has been introduced and then removed, tend to form only for regular or nearly regular connectivity (small values of q). Fig. 3A exemplifies this behavior for a network with $k = 41$ connections per unit, $\rho = 0.25$ and different values of q . In the example, a robust single bump forms for $q = 0$ and $q = 0.2$. A double bump forms for $q = 0.4$, and is relocated to a different section of the ring following the cue. A very noisy triple bump is barely noticeable towards the end of the simulation for $q = 0.6$, and no bumps can be really observed for random or nearly random nets, $q = 0.8$ and $q = 1$. Thus bump formation appears to be strongly favored by a regular connectivity, as expected.

3.3 Memory Retrieval in a Random Network

Fig. 3B shows the overlaps with the different memory patterns in the same simulations used for Fig. 3A, with $k = 41$. The cue which is presented after $150msec$ is correlated with the second pattern along one fourth of the ring, and it reliably enhances the overlap with the second pattern during cue presentation, whatever the value of q . By chance, the second (and to some extent the fifth) pattern tends to have an elevated initial overlap also before the presentation of the cue, a behaviour often observed in autoassociative nets and due to fluctuations. Despite this early 'advantage', once the pattern specific cue has been completely removed (after $500msec$, that is after the first 10 frames in the Figure) the overlap with the cued pattern returns to chance level, except in the case of a fully random ($q = 1$) or nearly random ($q = 0.8$) connectivity. Thus the randomness in the connectivity appears to favor memory retrieval, as expected, presumably by ensuring a more rapid propagation of the retrieval signal to the whole network, along shorter mean paths.

3.4 Bumps and Memory in Networks of Different Degrees of Order

Fig. 4 summarizes the results of simulations like those of Fig. 3, for $k = 41$ and a *fully extended* cue ($\rho = 100\%$). The spontaneous activity bumps, which are formed in the regular network, can be observed, somewhat reduced, up to $q \approx 0.4 \div 0.5$. For larger values of q the bumpiness measure quickly drops to a value close to zero. Storing random binary patterns on the network does not affect the bumps, but the retrieval performance appears to be very poor for small q , though the overlap measure with the pattern to be retrieved remains marginally above chance. As the randomness increases ($q \geq 0.6$), robust retrieval appears even though the normalized overlap is far from its maximum at 1. Still, for this value of the number of connections ($k = 41$), and for full cues, the transitions from bumps to no bumps and from no retrieval to retrieval both appear to be fairly sharp, and both occur between $q = 0.4$ and $q = 0.6$.

Results are somewhat clearer when considering partial cues, as shown in Fig. 5, which reports the retrieval measure averaged over all 5 cued patterns and over 10 network realizations, and as a function of cue quality. Despite the considerable variability (see the large standard deviations), the average retrieval performance appears to depend smoothly on q and ρ . For partial but still sufficiently large cues, $75\% \geq \rho \geq 25\%$, the network retrieves reasonably well when it is regular or nearly regular, $q \geq 0.7$, approaching the performance obtained with full cues. The overlap is reduced for $q = 0.6$, and it approaches zero for $q \leq 0.5$. For $\rho = 15\%$, retrieval appears for larger q and is weaker, and for even lower cue quality, $\rho = 5\% - 10\%$, essentially no retrieval occurs.

The non-zero average overlap measures reached by regular networks with full cues presumably reflect the network occasionally *freezing*, i.e. getting stuck in

a particular firing configuration, what may be called remnant magnetization in a spin system. This makes the distinction between retrieval and no retrieval somewhat fuzzier. Nevertheless, whatever the size of the cue, it is apparent that there is a well defined transition between two behaviors, bump formation and retrieval, which for $k = 41$ is concentrated between $q = 0.5$ and $q = 0.6$. The region of coexistence, if it exists, is in this case very limited.

Changing k does not affect the qualitative network behavior, as shown in Fig. 6 for the case of full cues and in Fig. 7 in the case of partial cues ($\rho = 50\%$). Whatever the connectivity k there is a transition between bump formation in nearly regular networks (on the left in each panel) and retrieval in nearly random networks (on the right). The transition is not always very sharp, and in some cases one could describe an individual network as able to both form bumps and retrieve memory patterns to some extent. When the number of connections is very limited ($k = 24$), both retrieval and bump formation are weak, when they at all occur. For more numerous connections the degree of bumpiness, as quantified by our measure, reaches for regular networks values close to 0.6 with full cues, and up to 0.75 with partial cues.

In Fig. 6, the range of the parameter of randomness, over which bump formation occurs, shrinks with increasing k , and in the case of $k = 208$ the bumpiness for $q = 0.2$ is already down to roughly 1/3 of its value for the regular network. The retrieval measure, instead, reaches higher values the larger the connectivity, approaching 1 for $k = 208$ and large q . In parallel to bump formation, the range of q values over which the network retrieves well appears to expand with k , so that for $k = 208$ essentially only regular networks fail to retrieve properly. Overall the transition from no retrieval to retrieval appears to occur in the same q -region as the transition from bumps to no bumps, and for the simulations with full cues reported in Fig. 6 this q -region shifts leftward, to lower q values, for increasing k .

The same lack of a region of coexistence between bump formation and retrieval is evident in Fig. 7, reporting simulations with partial cues, $\rho = 50\%$. Again, the bumpiness measure and more prominently the retrieval measure increase with more connections per unit, reflecting the larger storage capacity of networks with more connections. In our simulations the number of patterns is always fixed at $p = 5$, and the limited size of the network does not allow a straightforward application of storage capacity calculations valid for large systems [13]. Still, networks with $k = 24$ appear to operate above their capacity, and also for larger k the beneficial effect of a more extensive connectivity is in any case reflected in higher values for the overlap with the retrieved patterns. The major difference with Fig. 6 is that with partial cues the location of the transition between bumps and retrieval does not appear to be much affected by k , hovering between $q = 0.45$ and $q = 0.6$. Moreover, for regular and nearly regular networks the normalized overlap does approach zero, without any remnant magnetization effect; this appears to ‘allow’ the bumpiness measure to approach higher values, suggestive of an active interference between the two phenomena.

Bump formation has indeed been analytically shown to lower the storage capacity of threshold-linear networks [13], and it makes sense that the converse be also true, that is that even partial retrieval (which implies a proportion of quiescent units in the would-be bump) should loosen the bump and weaken its localization.

These results of both Fig. 6 and Fig. 7 contradict the expectation that one or both of these transitions be simply related to the small-world property of the connectivity graph. As shown above, the normalized value of the clustering coefficient, whose decrease marks the right flank of the small-world regime, is essentially independent of k , as it is well approximated, in our model, by the simple function $(1 - q)^3$. The transition between a localization regime and a retrieval regime, instead, to the extent that it can be defined for full cues (with the remnant magnetization artefact) clearly depends on k ; while for partial cues it occurs at a degree of randomness clearly beyond the small world range. The transition does not, therefore, simply reflect a small-world related property.

4 Discussion

Although small-world networks have been recently considered in a variety of studies, the relevance of a small-world type of connectivity for associative memory networks has been touched upon only in a few papers. Bohland and Minai [6] compare the retrieval performance of regular, small-world and random networks of an otherwise classic Hopfield model with binary units. They conclude that small-world networks with sufficiently large q approach the retrieval performance of random networks, but with the advantage of a reduced total wire length. Note that wire length is measured taking the physical distance between connected nodes into account, while path length is just the number of nodes to be hopped on in order to connect from one to another node of a pair. This result of reduced wire length for similar performance is likely quite general, but it relies on the small-world property of the connectivity graph only in the straightforward sense of using up less wiring (which is true also for values of q above those of the small-world regime); and not in the more non-trivial sense of using also the high clustering coefficient of small-world networks. The second result obtained by Bohland and Minai is that small-world nets can 'correct' localized errors corresponding to incomplete memory patterns quicker than more regular networks (but slower than more random network). This again illustrates behavior intermediate between the extremes of a well performing associative memory network with random connections, and of a poorly performing associative memory network with regular connections.

McGraw and Menzinger [10] similarly compare the final overlap reached by associative networks of different connectivity, when started from a full memory pattern (this they take to be a measure of pattern stability) and from a very corrupted version of a memory pattern (this being a measure of the size of a basin of attraction). In terms of both measures small worlds again perform

intermediate between regular and random nets, and in fact more similarly to random nets for values of $q \simeq 0.5$, intermediate between 0 and 1. They go on to discuss the property of another type of connectivity, the scale-free network, in which a subset of nodes, the 'hubs', receive more connections than the average, and therefore unsurprisingly performs better on measures of associative retrieval restricted to the behavior of the hubs themselves.

In summary, neither of these studies indicates a genuine non-trivial advantage of small-world connectivity for associative memories.

In our study, we considered integrate-and-fire units instead of binary units, so as to make more direct contact with cortical networks. More crucially, we also investigated, besides associative memory, another behavior, bump formation, or localization, which can also be regarded as a sort of emergent network computation. Morelli et al in a recent paper [12] study a seemingly analogous phenomenon, i.e. the emergence, in an associative memory with partially ordered connectivity, of discrete domains, in each of which a different memory pattern is retrieved. Although broadly consistent with our findings insofar as retrieval goes, the phenomenon they study is almost an artefact of the binary units used in their network, while we preferred to consider emergent behavior relevant to real networks in the brain. We wondered whether connectivity in the small-world regime might be reflected in an advantage not in performing associative retrieval alone, but in the coexistence of retrieval and bump formation.

The possibility of such a coexistence is precisely the question that was addressed in a recent study that focused on analytically-tractable networks of threshold-linear units [13]. While the connectivity model was different (it had a Gaussian spread with varying width) and unrelated to the notion of small-worlds, that study found that retrieval states can indeed be localized, even in regular networks, at the price of a relatively minor decrease in storage capacity. The very feature that makes threshold-linear units amenable to a full mathematical analysis, the lack of saturation in their output, may however subtract from the generality of the above results. In fact it was noted by Yasser Roudi (personal communication) that the units at the center of a *retrieval bump* need to be activated to much higher levels than those at its flanks with similar target activation in the memory pattern, or than the very same units when they participate in a non-localized retrieval state. Localized retrieval therefore requires the availability of a broad continuous range of activation levels (in the case of models with simple input-output units), and it cannot occur with binary units, or even with sigmoidal units in which active units all give essentially the same output.

In our present model, we used biologically more relevant integrate-and-fire units, whose firing rate, as a function of their inputs, follows, with more complex dynamics, a roughly intermediate behaviour between binary and threshold-linear. The absolute refractory period results in a saturation rate (in our case at

330Hz), but this ceiling is approached smoothly, and one has to understand whether units can use the wide range of firing levels to accommodate retrieval specificity within spatially localized states. We failed to observe this coexistence in practice, as networks go, with increasing randomness parameter q , from a localization regime with no (or very poor) retrieval - to a retrieving regime with no bumps. Further, we found that the critical transition q values are beyond the boundaries of the small-world region.

Because of its simulational character, our study cannot be taken to be exhaustive. For example, the partial retrieval behavior occurring for small q might in fact be useful when sufficiently few patterns are stored, p small. In our simulations, $p = 5$, but then the whole network was limited in size and connectivity. Moreover, a 2D network, which models cortical connectivity better than our 1D ring, might behave differently. Further, memory patterns defined over only parts of the network, which again brings one closer to cortical systems, might lead to entirely different conclusions about the coexistence of bump formation and associative retrieval. Our simulations, in any case, indicate the importance of considering a realistic model of input-output neuronal transform while addressing the issue of how to combine autoassociative memory retrieval with localization on a cortical map, an issue of crucial importance to understand the functions and microcircuitry of the cerebral cortex [15].

Acknowledgments

We are grateful to Francesco P. Battaglia and Haim Sompolinsky for their help at the early stage of the project; to Yasser Roudi for extensive discussions of his work; to the EU Advanced course in Computational Neuroscience (Obidos, 2002) for the inspiration and opportunity to develop the project; and to the Burroughs Wellcome Fund for partial financial support.

References

- [1] D. J. Amit, N. Brunel, Dynamics of a recurrent network of spiking neurons before and following learning, *Network* **8** (1997) 373-404
- [2] F. P. Battaglia, A. Treves, Attractor neural networks storing multiple space representations: A model for hippocampal place fields, *Physical Review E* **58** (1998a) 7738-7753
- [3] F. P. Battaglia, A. Treves, Stable and rapid recurrent processing in realistic autoassociative memories, *Neural Computation* **10** (1998b) 431-450
- [4] R. Ben-Yishai, R. Lev Bar-Or, H. Sompolinsky, Theory of orientation tuning in visual cortex, *Proc Natl Acad Sci USA* **92** (1995) 3844-3848
- [5] E. Bienenstock, On the dimensionality of cortical graphs, *J Physiology-Paris* **90** (3-4) (1996) 251-25
- [6] J. W. Bohland, A. A. Minai, Efficient associative memory using small-world architecture, *Neurocomputing* **38** (2001) 489-496
- [7] B. Bollobas, Random Graphs, *Academic Press, New York* (1985)
- [8] B. Derrida, E. Gardner, A. Zippelius, An exactly soluble asymmetric neural network model, *Europhysics Letters* **4** (1987) 167-174
- [9] J. J. Hopfield, Neural networks and physical systems with emergent collective computational abilities, *Proc Natl Acad Sci USA* **79** (1982) 2554-2558
- [10] P. N. McGraw, M. Menzinger, Topology and computational performance of attractor neural networks, *Phys Rev E* **68** (2003) Art.047102
- [11] S. Milgram, The small-world problem, *Psychol. Today* **2** (1967) 60-67
- [12] L. G. Morelli, G. Abramson, M. N. Kuperman, Associative memory on a small world neural network, *Eur Phys J B* **38** (2004) 495-500
- [13] Y. Roudi, A. Treves, An associative network with spatially organized connectivity, *J Stat Physics* **1** (2004) P07010
- [14] A. Treves, Mean-field analysis of neuronal spike dynamics, *Network* **4** (1993) 259-284
- [15] A. Treves, Computational constraints that may have favoured the lamination of sensory cortex, *J Comput Neurosci* **14** (2003) 271-282
- [16] M. V. Tsodyks, M. V. Feigl'man, The enhanced storage capacity in neural networks with low activity level, *Europhysics Letters* **6** (1988) 101-105
- [17] H. C. Tuckwell, Introduction to theoretical neurobiology, *Cambridge University Press, New York NY* (1988)

- [18] D. J. Watts, The dynamics of networks between order and randomness, *Princeton University Press, Princeton NJ* (1999)
- [19] D. J. Watts, S. H. Strogatz, Collective dynamics of 'small-world' networks, *Nature* **393** (1998) 440-442

Figure 1: (A) Numerical results for the normalized characteristic path length $L'(q) = [L(q) - L_{min}]/[L_{max} - L_{min}]$ and the normalized clustering coefficient $C'(q) = [C(q) - C_{min}]/[C_{max} - C_{min}]$ as a function of the parameter of randomness (averaged over 10 network realizations, all with the same number $k = 41$ of outgoing connections per neuron). Inset: logarithmic x-scale showing the small world regime for small q . (B) Comparison of the analytical and numerical results for the clustering coefficient C (not normalized, $k = 41, N = 1000$).

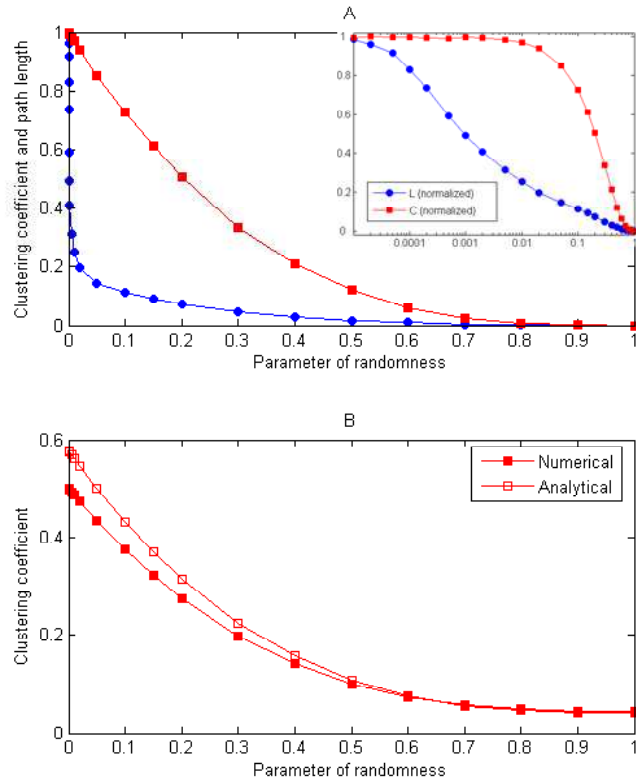


Figure 2: Spontaneous emergence of a bump in the activity profile of a regular network ($q = 0$) with an average number of outgoing connections per neuron $k = 41$.

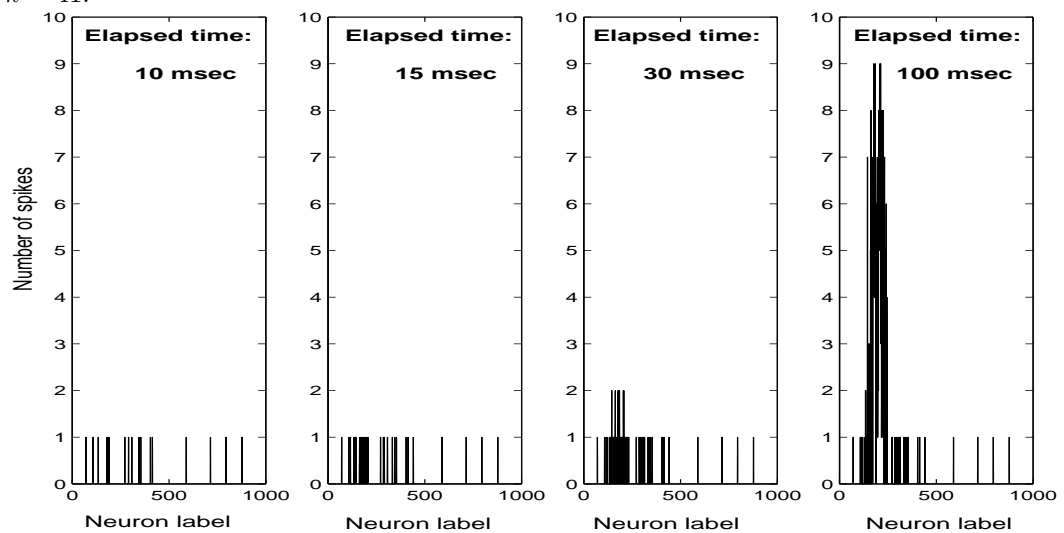


Figure 3: (A) Activity profiles during the simulation for different values of the parameter of randomness. Shown is the number of spikes r_i (vertical axis) that each neuron (horizontal axis) has fired in a sliding 50 msec time window. (B) Overlaps O^μ (vertical axis) of the network activity shown in (A) with each of the $p = 5$ previously stored memory patterns (horizontal axis) - before, during, and after a 25%-quality cue for the pattern $\mu = 2$ has been given.

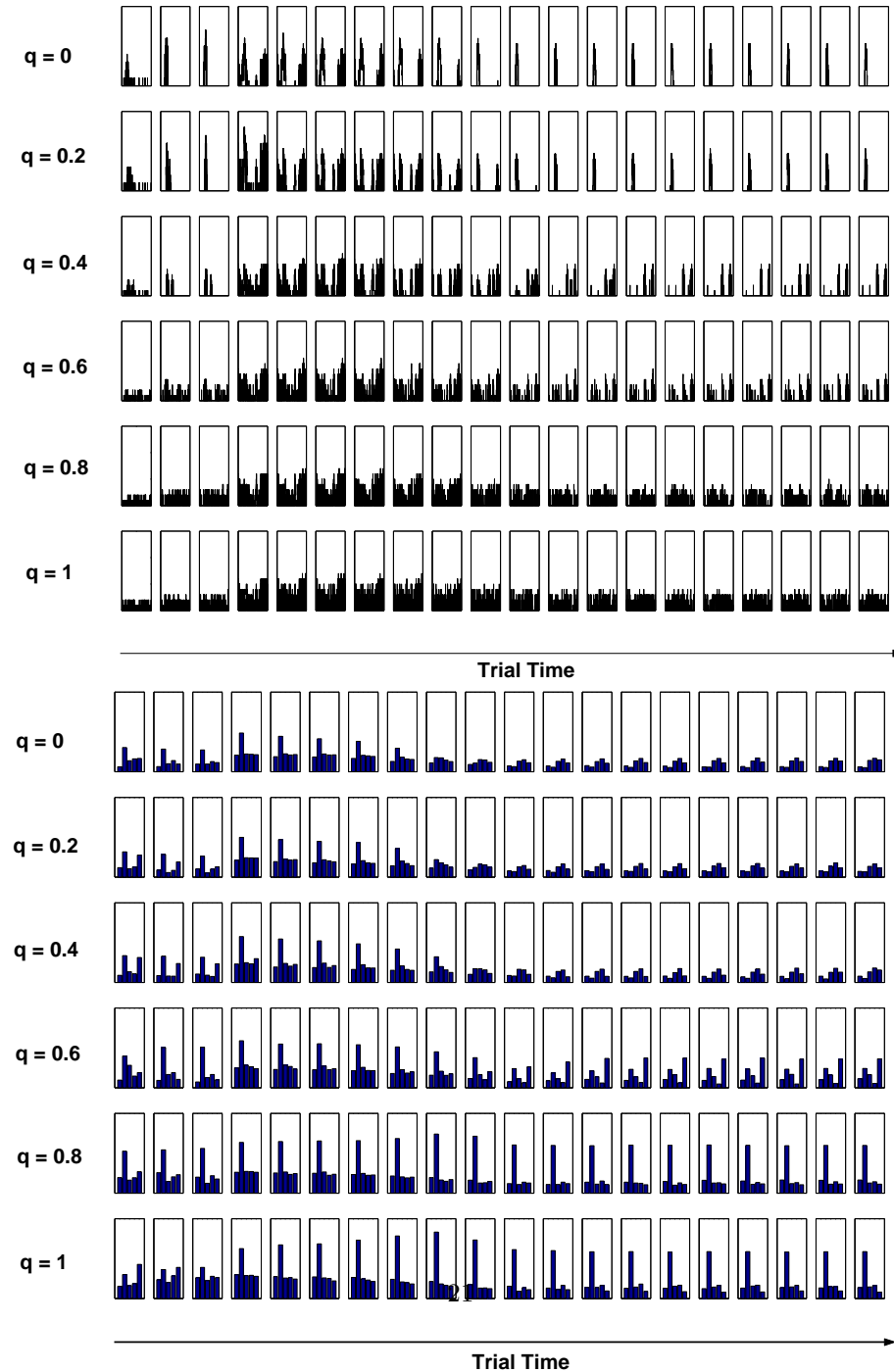


Figure 4: Bumpiness of the activity profile (A) and retrieval performance (B) as a function of the parameter of randomness for the average of 10 network realization, with $k = 41$ and $\rho = 1$ (error bars are report the stadard deviation across realizations).

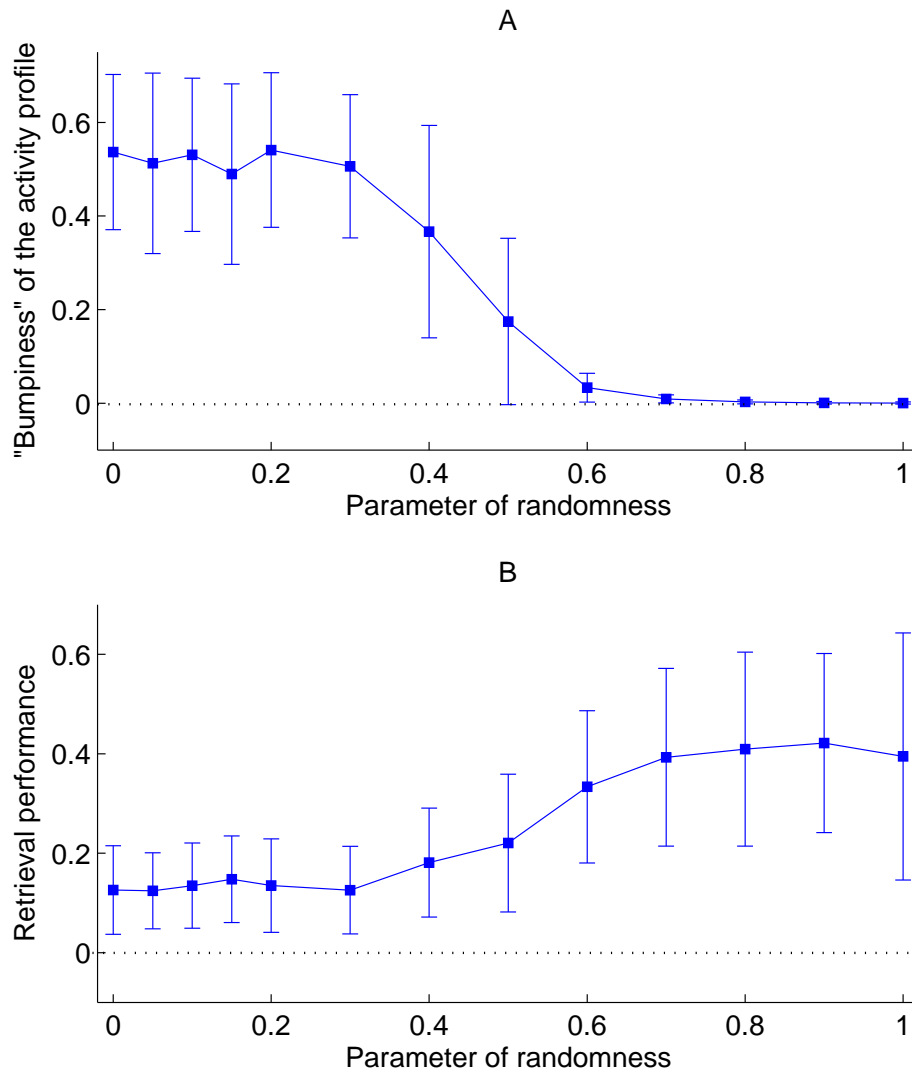


Figure 5: The effect of the cue quality ρ (displayed in the legend) on retrieval performance, for the average of 10 network realizations with $k = 41$.

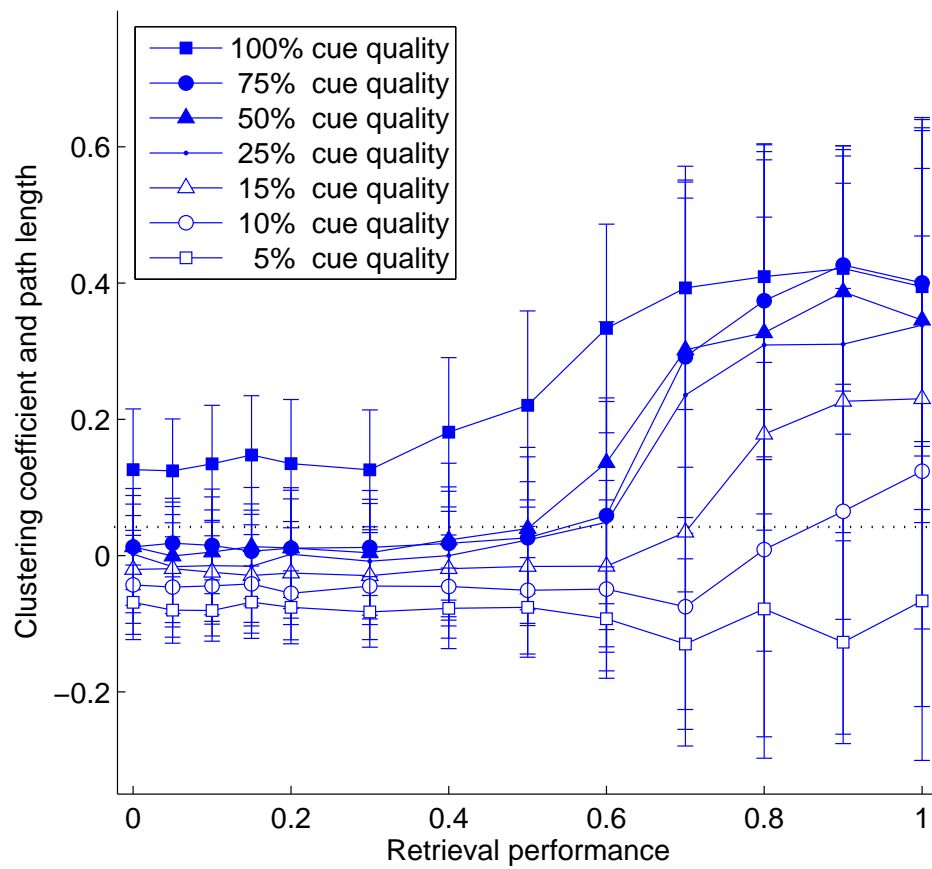


Figure 6: The effect of changing the number k of connections per neuron on the retrieval performance (triangles) and on the bumpiness (dots), for full cues.

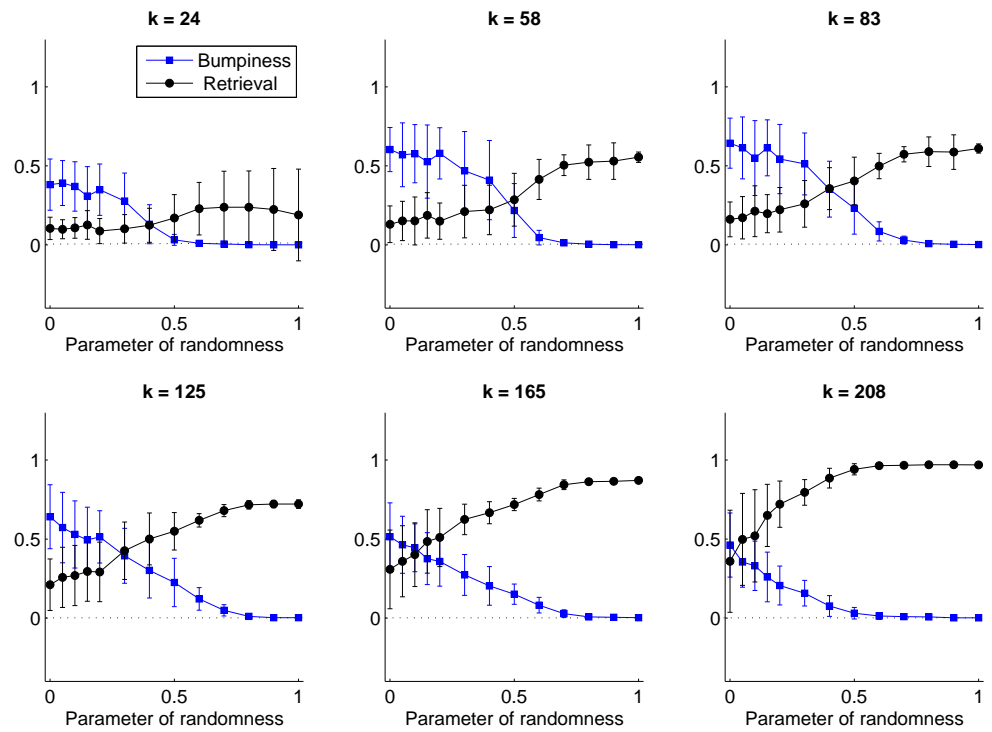


Figure 7: The effect of changing the number k of connections per neuron on the retrieval performance (triangles) and on the bumpiness (dots), for partial cues, $\rho = 50\%$.

